DEÜ FMD 25(75), 739-750, 2023

1

Dokuz Eylül Üniversitesi Mühendislik Fakültesi Fen ve Mühendislik Derg
Dokuz Eylul University Faculty of Engineering Journal of Science and En

Basılı/Printed ISSN: 1302-9304. Elektronik/Online ISSN: 2547-958X

Site Response Predictions at Atakoy Downhole Array

Ataköy Gözlem Kuyusunda Saha Tepki Tahminleri

Yusuf Guzel [1*], Fidan Guzel [2]

Necmettin Erbakan University, Engineering Faculty, Konya, TÜRKİYE
[2] Igdir University, Engineering Faculty, Igdır, TÜRKİYE
Sorumlu Yazar / Corresponding Author *: yusufkurtdereli@hotmail.com

Geliş Tarihi / Received: 07.11.2022 *Araştırma Makalesi/Research Article*
Kabul Tarihi / Accepted: 25.04.2023 *DOI:10.21205/deufmd.2023257517*
Atıf şekli/ How to cite: GUZEL, Y., GUZEL, F. (2023). Site Response Predictions at Atakoy Downhole Array. DEUFMD, 25(75), 739-750.

Abstract

Site response analyses are seen to be the reliable way of reproducing and predicting earthquake input motions. The analyses are generally performed by adopting equivalent linear or nonlinear approaches solving the problem in time or frequency domains. Instrumented geotechnical downhole arrays, in this regard, are very important as to obtaining earthquake data through the soil deposits. This data can eventually be used to verify the approaches developed for site response analyses. In this study, the input motions of the 24.05.2014 (Aegean) earthquake event recorded at relatively recently installed Atakoy geotechnical downhole array are assessed. Moreover, the recorded input motions at the bottom bedrock level of the downhole array are simulated in the East-West and North-South directions. The site response analyses are conducted based on frequency domain equivalent linear approach. The peak ground acceleration and the spectral accelerations of the predicted input motions are compared with the recorded ones at 70 m, 50 m, 25 m and at the ground surface. The results indicate that the spectral acceleration predictions can be simulated well until the depth of 50 m. At 25 m and at ground surface, the predictions are always greater than the recorded one. However, the predictions still exhibits good indication of actual values in the North-South direction. In terms of peak ground acceleration and shear strain profiles, the predictions display the soil layers featured with different soil properties. The equivalent linear approach appears to be suited reasonably well in site response analysis.

Keywords: Site Response Analysis, Downhole Arrays, Earthquake Input Motions, Spectral Response Predictions

Özet

Saha davranış analizleri deprem ivme hareketlerini yeniden üretmede ve tahmin etmede kullanılabilecek bir yöntem olduğu benimsenmiştir. Saha analizleri, genellikle, problemi zaman veya frekans bazda çözen eşdeğer doğrusal veya doğrusal olmayan yaklaşımlar benimsenerek gerçekleştirilir. Enstrümanlı geoteknik gözlem kuyuları bu açıdan zemin tabakaları boyunca hareket eden deprem ivme değerlerinin elde edilmesi açısından oldukça önemlidir. Bu veriler nihayetinde saha davranış analizleri için geliştirilen yaklaşımları doğrulamak için kullanılabilir. Bu çalışmada, nispeten yakın zamanda kurulmuş Ataköy geoteknik kuyusunda kaydedilen 24.05.2014 (Ege) depreminin ivme hareketleri değerlendirilmiştir. Ayrıca, kuyuanakaya seviyesinde kaydedilen ivme hareketleri Doğu-Batı ve Kuzey-Güney yönünde simüle edilmiştir. Saha davranış analizleri, frekans bazlı eşdeğer doğrusal yaklaşıma dayalı olarak yürütülmüştür. Tahmin edilen ivme hareketlerinin maksimum yer ivmesi ve spektral ivmeleri, 70 m, 50 m, 25 m ve zemin yüzeyinde kaydedilen değerler ile karşılaştırılmıştır. Sonuçlar, spektral ivme tahminlerinin 50 m derinliğe kadar iyi bir şekilde simüle edildiğini göstermektedir. 25 m'de ve zemin yüzeyinde, tahmin edilen değerler kaydedilen değerlerden her zaman daha büyük olarak elde edilmektedir. Bununla birlikte, tahminler hala Kuzey-Güney yönündeki gerçek değerlere yakın olduğunu göstermektedir. Maksimum yer ivmesi ve birim şekil değiştirme profilleri açısından, tahminler farklı zemin özelliklerine sahip zemin tabakalarını yansıtmaktadır. Eşdeğer doğrusal yaklaşımın, saha davranış analizi için uygun bir yöntem olduğu görünmektedir.

AnahtAnahtar Kelimeler: *Saha Davranış Analizi, Geoteknik Gözlem Kuyuları, Deprem Zemin İvme Kayıtları, Spektral İvme Tahminleri*

1. Introduction

One of the known natural hazards that causes great amount of economical losses, most substantially, human casualties, is known as earthquakes. Hazards of such natural event to urban areas are shown dependency to the peak ground acceleration (PGA) levels reaching to the site [1]. The level of PGA dissipates within the rock and soil bodies by distances from the epicenter of an earthquake events. Therefore, seismicity of any site depends on its position relative to the earthquake fault lines [2-4].

The characteristics of seismic input motions are mainly influenced by three factors until they reaches to the ground surface. These factors can be listed as fault mechanism, path and site effects [5]. In order to reflect site effect, site response analysis can be conducted. Moreover, predicting input motions at the ground surface is very important for the design of buildings in seismically active regions. Hence, simulating the seismic input motions through the soil deposits can guide engineers with respect to better include the ground input motions, in their designs [6, 7].

Site response analyses are solved through the equivalent linear or nonlinear methods in frequency or time domains [8, 9]. In order to verify that the developed site response method can able to give reliable predictions, actual earthquake data recorded through the soil deposits is needed. In this respect, geotechnical downhole arrays that are instrumented have been settled at several seismically active regions.

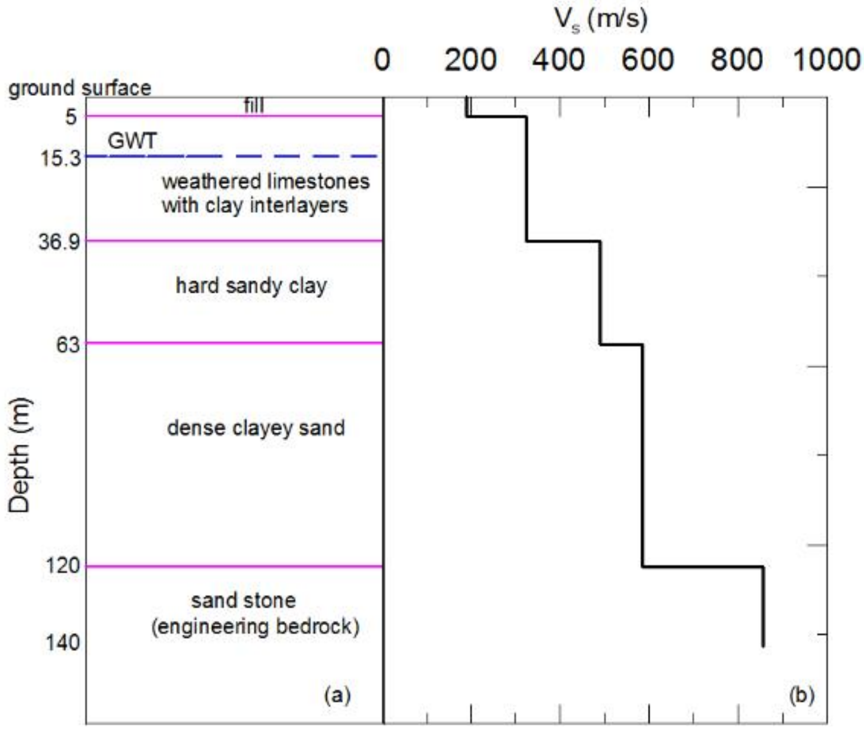

Figure 1. (a) Geological formations at the site of Atakoy downhole array, (b) shear wave velocity profile until the engineering bedrock at the 140 m depth [17]

For instance, Lotung geotechnical array [8, 10-11], Treasure Island geotechnical array [12-13], Parkfield- Turkey flat [14-15] and La Cienega geotechnical array [11] are some of the well-known geotechnical arrays among others. The earthquake data collected at these arrays were used to test the equivalent linear and nonlinear site response approaches, involving advanced soil models in several studies.

In this study, one of the geotechnical arrays instrumented recently in Istanbul, Atakoy, is considered. In particular, the input motion recordings of the Aegean earthquake event at the different depths of the array are assessed and simulated. The array is modelled with full depth of 140 m. The performance of the frequency domain site response approach is evaluated in terms of spectral accelerations, PGA and shear strain profiles. It is important to note that this study differs from the study of [16] in two ways; it fully models the soil deposit (i.e. the Atakoy downhole array) for the first time and predicts the input motions at different depths through site response analysis. However, the aforementioned study only assesses the recorded input motions from the Aegean earthquake event at the Atakoy downhole array and at other two downhole arrays (i.e. Fatih and Zeytinburnu downhole arrrays).

2. Atakoy Downhole Array

Atakoy downhole array is located in the west side of Istanbul, close to the Ataturk airport. It has been opened up in 2005 for a research project operated by Kandilli Observatory and Earthquake Research Institute of Bogazici University (KOERI) cooperating with German Research Center for Geosciences (GFZ) [17].

The underlain engineering bedrock were produced during Eocene age Ceylan formation. The sand and clay layers along with the limestone layer were formed with Güngören formation within the Miocene period (as seen in Figure 1a). Specifically, below 140 m, the engineering bedrock exists when between 140 m and 120 m the sand stone soil layer is encountered. Above sand stone layer, dense clayey soil is situated until 63 m, overlaid by hard sandy clay until 36.9 m. Between 36.9 m and 5 m, weathered limestones with clay interlayers is positioned, above which recently formed fill layer stretching to the ground surface. The ground water table is thought to be at the depth of 15.3 m [16].

In order to gather data in relating with possible earthquake events around the site, the downhole array was instrumented. Particularly, accelerometers were positioned at 140 m, 70 m, 50 m and 25 m depths and at the ground surface. The shear wave velocity (V_s) values at the downhole array were obtained from PS suspension logging tests, as presented in Figure

Figure 2. Locations of the epicentre of the Aegean earthquake event and the Atakoy downhole array

1b. While the fill layer has V_s of 188 m/s, underlain limestone layer has V_s of 323 m/s. Following sandy clay and sand soil layers have V_s of 490 m/s and 586 m/s, respectively. As the overall average V_s value of the soil deposit is 532.55 m/s, that value at the top 30 m is 300 m/s. therefore, the site can be classified as soil class ZD according to Turkish Building Design Code [18] and as soil class C according to Eurocode 8 [19].

3. Recordings at the Downhole Array

Between the years of 2006 and 2010, several small magnitude (≤ 5.0) earthquake events were recorded [16]. In addition, on 24th of April, in 2014, the earthquake event (known as Aegean earthquake event) with moment magnitude of 6.9 was recorded at the downhole array. The locations of the event and the Atakoy downhole array are represented in Figure 2 [20]. The coordinate of the epicentre of the earthquake event is 40.2108^0 latitude and 25.3073^0 longitude and the coordinate of the Atakoy downhole array is 40.9819^0 latitude and 28.8392^0 longitude. Bird eye distance from the epicentre to the downhole array is approximately 313.73 km.

In this research, recordings of the earthquake event along the downhole array are considered during the site response analyses. Recorded input motions of the earthquake event at the engineering bedrock level (i.e. 140 km) in the East-West (E-W) and North-South (N-S) directions are represented in

Figure 3a and Figure 3b, respectively. While the PGA level in the E-W direction is 0.039 m/s^2, this value equals to 0.046 m/s^2 in the N-S direction. The corresponding spectral acceleration values of the bedrock level input motions are also demonstrated in Figure 3c and Figure 3d. This is for the reason of indicating spectral shape of the input motions, which has already travelled through the bedrock body, reaching to the site, which reflect the energy content concentration over the periods. The recorded input motions within the downhole array in the E-W and N-S directions at the ground surface, 25 m, 50 m and at the 70 m depths are also shown in Figure 4a-b, Figure 4c-d, Figure 4e-f and Figure 4g-h, respectively.

The PGA values of the recorded earthquake input motions at different depths and at the ground surface in both horizontal directions and in the up-down (U-D) direction are displayed in Table 1. It is clear that from the depth of 140 m to 70 m, the PGA values are almost doubled from 0.039 m/s^2 to 0.079 m/s^2 in the E-W direction and from 0.046 m/s^2 to 0.086 m/s^2 in the N-S direction. However, when the input motions travelled towards the hardly sandy clay soil layer from the dense clayey sand, the PGA values in both horizontal directions are deamplified. From the sandy clay soil layer to the limestone one and ultimately to the ground surface, the input motions in both horizontal directions (as well as U-D direction) amply. More specifically, the PGA value in the E-W direction gets to 0.08 m/s^2 (from 0.0716 m/s^2 at the 50 m depth) at the 25 m depth and to the value of 0.088 m/s^2 at the ground surface. In the N-S direction, these values at the aforementioned depths become 0.088 m/s^2 and 0.112 m/s^2 (from 0.0763 m/s^2 at the 50 m depth), respectively.

Table 1. PGA values of the recorded input motions at the Atakoy downhole array at the ground surface, 25 m, 50 m, 70 m and 140 m depths in the E-W, N-S and U-D directions

Directions / Depth (m)	PGA (m/s^2)		
	E-W	N-S	U-D
Ground surface	0.088	0.112	0.040
25	0.08	0.088	0.039
50	0.0716	0.0763	0.036
70	0.079	0.086	00347
140	0.039	0.046	0.026

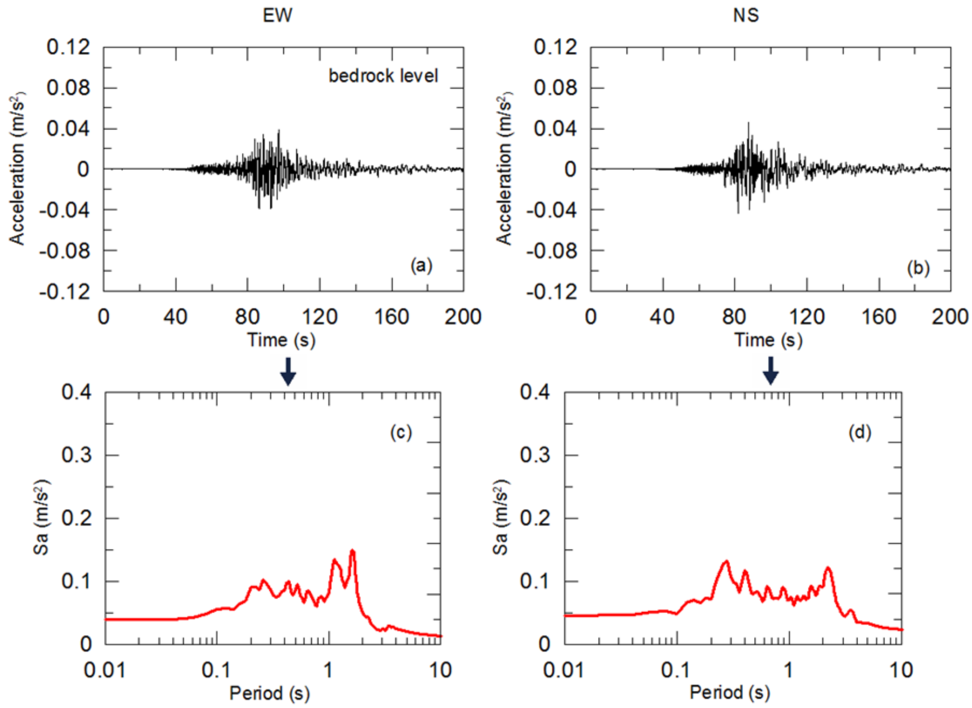

Figure 3. Recorded input motions at the bedrock level: (a) in the E-W direction (b) in the N-S direction and corresponding spectral acceleration curves (c and d, respectively) (16)

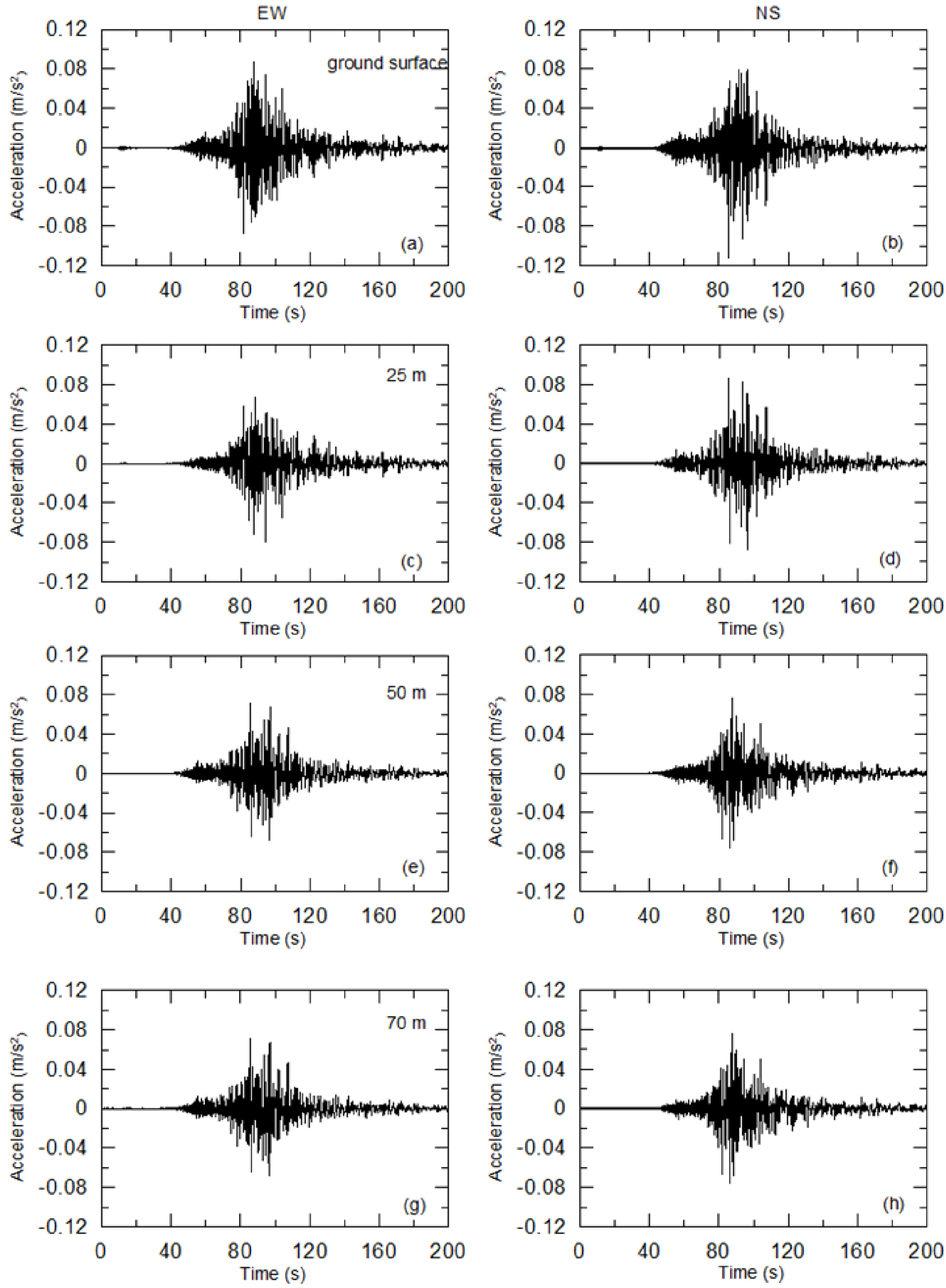

Figure 4. Recorded earthquake input motions at the ground surface (a and b), 25 m (c and d), 50 m (e and f) and at the 70 m (g and f) depths in both horizontal directions (in order of E-W and N-S)

4. Soil Modelling

In site response analyses, modelling of the soil layers in a studied are is very critical. Because, in order to get reliable predictions from the site response analyses, the characteristics of soil layers should rigorously be determined. Initial stiffness profile (V_s) and the reduction of initial shear modulus (G/G_0) and corresponding damping ratios (D, %) by the increase of the shear strain are two main components in the site response analyses having great impact on the site response predictions.

The Atakoy downhole array is modelled in DeepSoil software [21] until the depth of 140 m (i.e., until the realised engineering bedrock). As stiffness profiles for each soil layer, the V_s values represented in Figure 1b are introduced. For the G/G_0 and D (%) curves, Seed and Idriss [22] standard curve (mean) for sandy soil layers and plasticity index (PI) based Vucetic and Dobry [23] standard curve for the clayey soil layers are adopted. Since, the V_s values between 120 m and 140 m are greater than 760 m/s (referring to Figure 1), which is a value separating the soil and rock, different G/G_0 and D (%) curves representing the more of rock behaviour are represented. More clearly, for fill (0-5 m), weathered limestone (5-36.9 m) and hard sandy clay, Vucetic and Dory curve given for the PI equals to 30 are introduced, as shown in Figure 5a-d. For underlain dense clayey sand (63-120 m), mean Seed and Idriss curve is assigned (Figure 5b-e). As for the sand stone layer (120-140 m), the G/G_0 and D (%) curves demonstrated in Figure 5c-f is involved. Since the Atterberg limit test and other laboratory test results to produce the G/G_0 and D (%) curves are not available in the literature, the average G/G_0 and D (%) curves given within the software are used. The site response analyses are carried out based on frequency domain equivalent linear approach. The bottom of the soil model is regarded as rigid.

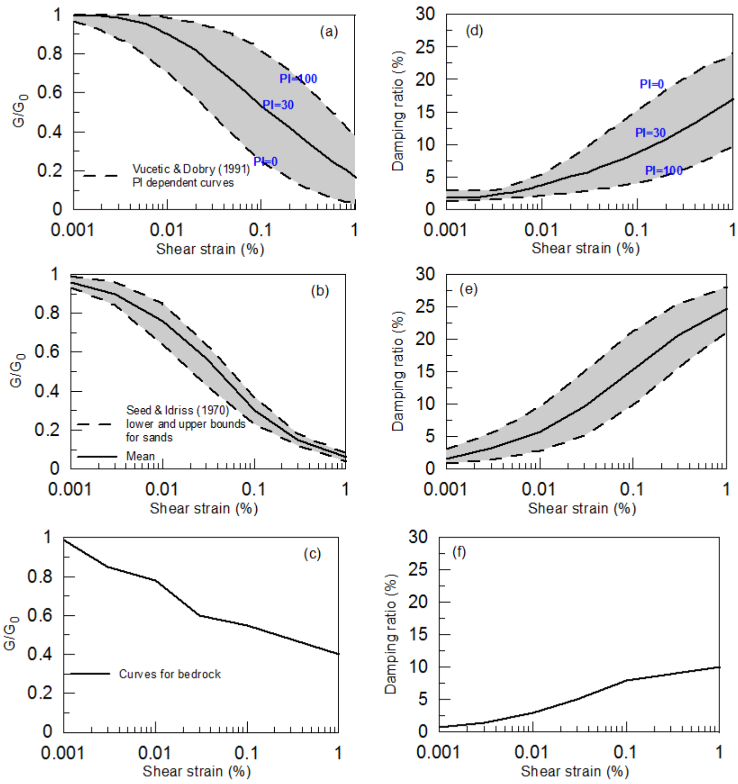

Figure 5. Shear modulus reduction (G/G0) curves (left column) for; (a) clayey soil layers, (b) sandy soil layers and (c) bedrock layer and corresponding damping ratio (D%) curves (right column) shown in (e), (f) and (g), respectively

5. Results and Discussions

The soil deposit modelled in the DeepSoil software with the total height of 140 m is simulated in the E-W and N-S directions, separately, under the recorded input motions presented in Figure 3a and in Figure 3b, respectively. The results of site response analyses are interpreted, specifically, in terms of spectral acceleration, PGA and shear strain predictions. While the spectral acceleration predictions along with the actual data at the ground surface, 25 m, 50 m and 70 m depths are presented in Figure 6. PGA and shear strain profiles including the actual PGA values are illustrated in Figure 7 and Figure 8, respectively.

It is clear that the equivalent linear site response predictions at the 70 m depth matches quite well with the actual recordings in the E-W and N-S directions (as can be seen in Figure 6g-h, respectively). At this depth, the PGA value and the spectral peaks occurring just around 1 s are well captured. When the input motions travels from 70 m to 50 m in the N-S direction (Figure 6e), the spectral peak still happens at 1 s with the value of 0.276 m/s^2, being lower than actual spectral peak value of 0.4 m/s^2 at 1.126 s. Moreover, a second spectral peak with almost same spectral value appears at the period of 0.4 s, which is not seen in the actual spectral acceleration curve. However, this second spectral peak predicted at 50 m (Figure 6f) disappears as the simulated input motion reaches to 25 m (Figure 6d) and appears again at the ground surface (Figure 6b). Nevertheless, the main actual spectral peak is predicted relatively good at 25 m and shows good proxy (even though larger than the actual spectral peak) at the ground surface.

When it comes to predictions in the E-W direction, the equivalent linear approach causes always greater spectral values than the actual values over the periods between 0.01 s and 2 s, especially at the depths of 50 m, 25 m and at the ground surface, as can be seen in Figure 6e-c-a, respectively. The diversion from the actual data is getting wider towards the ground surface and is particularly pronounced between 0.945 s and 1.53 s, within which the main spectral peaks take place. More precisely, at 50 m, the actual spectral peak is 0.26 m/s and predicted spectral peak is 0.574 m/s^2 occurring at 1.14 s (Figure 6e). At 25 m, the actual spectral peak value equals to 0.27 m/s^2 at 1 s, and predicted one is 0.72 m/s^2 at 1.11 s (Figure 6c). Ultimately, at the ground surface, the actual spectral peak becomes 0.34 m/s^2 at 1 s, and predicted one gets to 0.81 m/s^2 at 1.12 s (Figure 6a). Second spectral peak also occurs in the simulated E-W input motion predicted at the ground surface that is again not observed in the recorded data (Figure 6a). The value of this second spectral peak equals to 0.434 m/s^2 at 0.44 s.

The recorded PGA values in the E-W direction seem to be well represented by the predictions from the site response analysis from the bottom of the model until 110 m (Figure 7a). However, from this depth up to the ground surface, the predicted PGA value increases almost linearly from 0.056 m/s^2 to 0.146 m/s^2. In contrast, the recorded PGA values (or PGA profile) are always lower than the predicted ones and fluctuate through the soil deposit. For instance, it increases from 0.056 m/s^2 at 110 m to 0.074 m/s^2 at 63 m, then reduces to 0.065 m/s^2 at 50 m. Subsequently, it increases to 0.089 m/s^2 at 25 m and to 0.1 m/s^2 at the ground surface. The predicted PGA values in the N-S direction tends to represent relatively well (although the predicted PGA values are smaller than the actual ones) the actual data up until 37 m (Figure 7b). Above this depth towards the ground surface, the predicted PGA values are always higher than the actual ones reaching to 0.126 m/s^2 as opposed to the actual recorded value being 0.086 m/s^2. The recorded PGA profiles in both horizontal directions tends to reflect the different soil profiles. This is also valid for the predicted PGA profile in the N-S direction, but cannot be expressed for the PGA profile in the E-W direction.

Accumulated shear strain profiles through the soil model simulated under the E-W and N-S input motions are illustrated in Figure 8a and in Figure 8b, respectively. It is clear that between 140 m and 120 m depths, the shear strain value in both cases does not change. Clear increase of shear strain values when the input motions are transported to the above soil layer is observed. However, within the same soil layer, the shear strain reduces in both directions. The maximum strain value is accumulated between hard sandy clay and weathered limestone soil layers at 36.9 m, which equalts to 0.06 (%) in the E-W direction and 0.044 (%) in the N-S direction. At the ground surface, the predicted shear strain values in the E-W and N-S directions become 0.002 (%) and 0.0017 (%), accordingly. Lastly, it

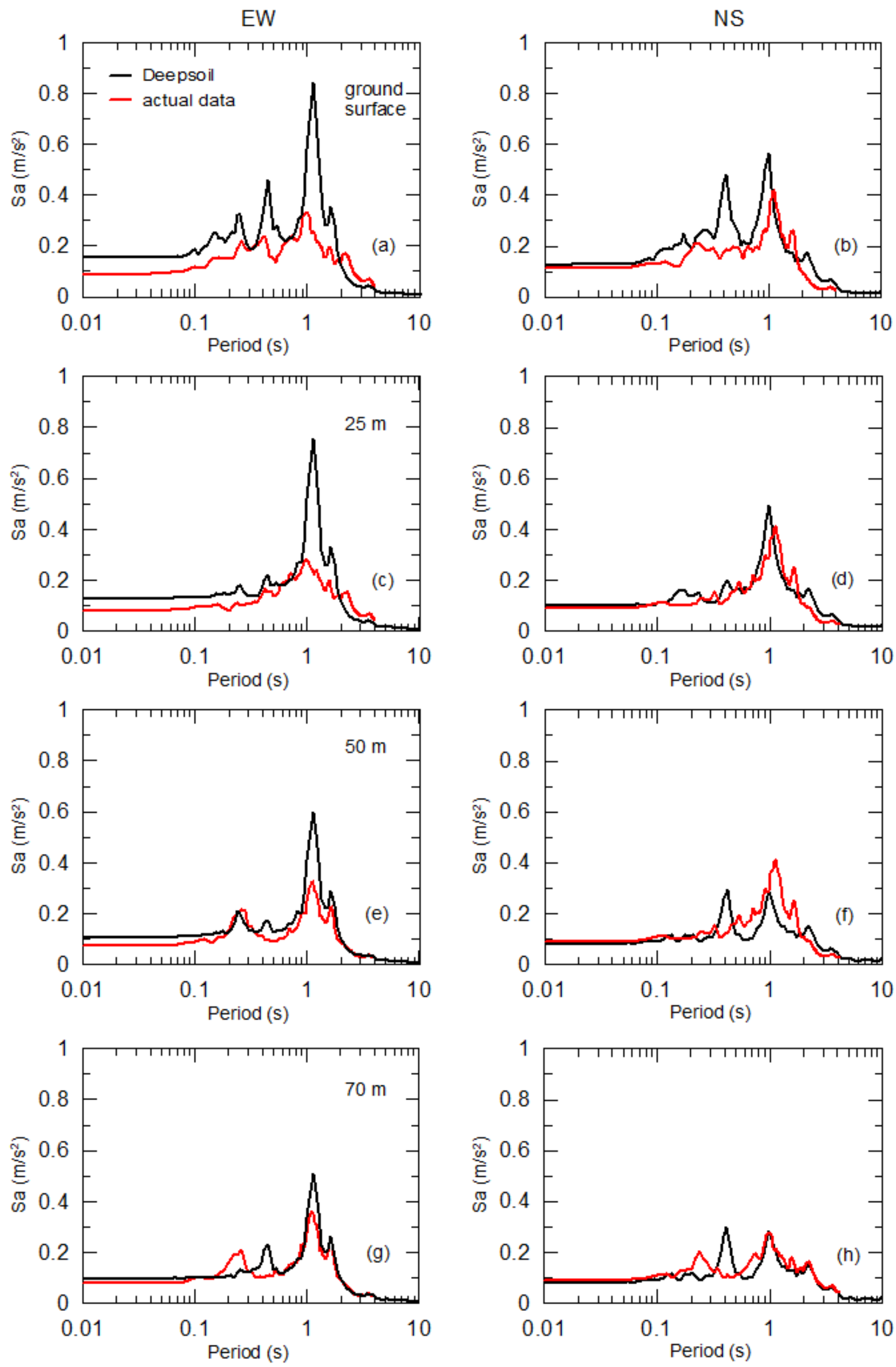

Figure 6. Spectral acceleration predictions compared with the actual recordings of spectral values (in the E-W and N-S directions) at; (a, b) the ground surface, (c, d) the 25 m depth, (e, f) the 5 m depth and (g, h) the 70 m depth

is clear that different types of soil layers can easily be seen in the PGA and shear strain profiles, indicating good performance of the equivalent linear approach in the site response predictions.

On the whole, the equivalent linear approach performs well in predicting spectral accelerations at the shorter (≤0.1 s) and at the longer periods (≥ 1 s or 2 s). In contrast, the approach cannot able to present the actual spectral acceleration values between 0.1 s and 1 s. This is particularly true for the predictions at the ground surface. In fact, the studies of [24] and [25] suggest that the equivalent linear approach can give reliable predictions at all period ranges until the shear strain level being equal to or less than 0.4 (%). Although, in this study, the accumulated shear strain reaches to the value of 0.044 (%), the predicted spectral acceleration values are not well matched with

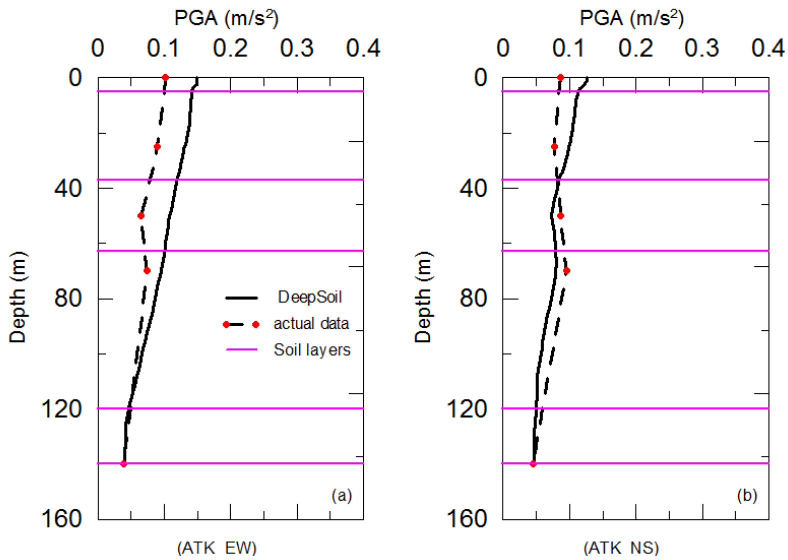

Figure 7. Recorded and predicted PGA profiles in the E-W (a) and N-S (b) directions through the downhole array

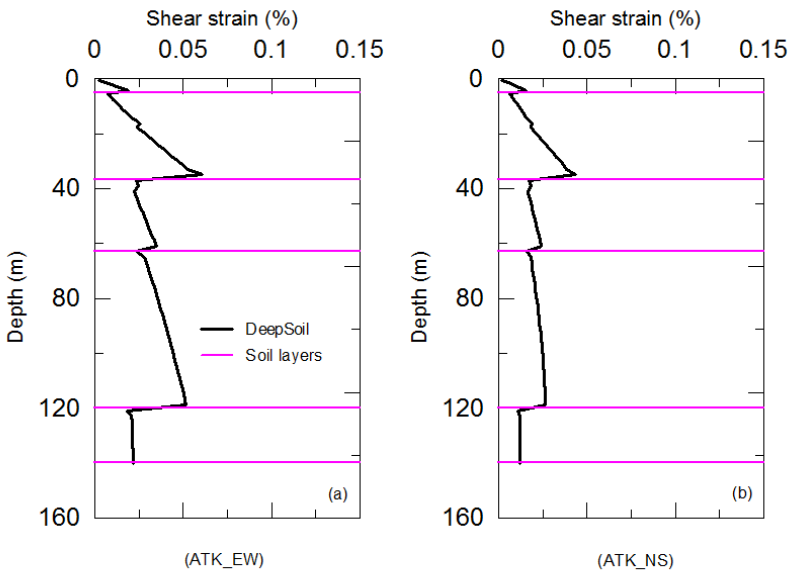

Figure 8. Predicted shear strain profiles along the downhole array in the E-W (a) and N-S (b) directions

the actual values at all period ranges. The discrepancy is pronunced more, in particular, at the 0.1 s and 1 s period ranges while at the shorter and longer periods the discrepacny is relatively insignificant.

6. Conclusions

In this study, recordings of the Aegean earthquake event (occurred on 24 of April, 2014) at the Atakoy downhole array are evaluated. Moreover, the recorded input motions in the E-W and N-S directions at the bedrock level of the downhole array are simulated, individually. The simulations are conducted by using DeepSoil software applying equivalent linear approach in frequency domain. The results of the site response analyses are represented in terms of spectral accelerations and PGA and shear strain profiles. The outcomes of this research can be listed as follows;

- The equivalent linear approach results in good spectral response predictions, in particular, in the N-S direction, capturing the period of spectral peaks as well as its absolute values at all recorded depths,
- The predicted PGA profiles reflect the different soil layers whose features have impact on the seismic input motions,
- Similarly, the shear strain profiles are characterised by the soil layers and getting smaller until reaching the ground surface.

Overall, the site response analysis seems to be promising way of predicting the actual seismic behaviour of the sites. The downhole array sites, as the one investigated in this research, provide reliable source of earthquake data at different depths, enabling to confirm the methods implemented in conducting site response analyses.

Acknowledgement

The author acknowledges the help of Prof. Erdal Şafak (at Bogazici University) in attaining the recorded data.

References

[1] Kramer, S. L. 1996. Geotechnical earthquake engineering. Pearson Education India.

[2] Idriss, I. 2014. An NGA-West2 empirical model for estimating the horizontal spectral values generated by shallow crustal earthquakes, Earthquake Spectra, vol. 30, no. 3, pp. 1155-1177. DOI: 10.1193/070613EQS195M

[3] Ambraseys, N. N., Douglas, J., Sarma, S., Smit, P. 2005. Equations for the estimation of strong ground motions from shallow crustal earthquakes using data from Europe and the Middle East: horizontal peak ground acceleration and spectral acceleration, Bulletin of earthquake engineering, vol. 3, no. 1, pp. 1-53. DOI: 10.1007/s10518-005-0186-x

[4] Campbell, K. W. 2003. Prediction of strong ground motion using the hybrid empirical method and its use in the development of ground-motion (attenuation) relations in eastern North America, Bulletin of the Seismological Society of America, vol. 93, no. 3, pp. 1012-1033. DOI: 10.1785/0120040148

[5] Guzel, Y. 2019. Influence of input motion selection and soil variability on nonlinear ground response analyses Newcastle University, Newcastle.

[6] Sextos, A., et al. 2018. Local site effects and incremental damage of buildings during the 2016 Central Italy Earthquake sequence, Earthquake Spectra, Article vol. 34, no. 4, pp. 1639-1669. DOI: 10.1193/100317EQS194M

[7] Gautam, D., Forte, G., Rodrigues, H. 2016. Site effects and associated structural damage analysis in Kathmandu Valley, Nepal, Earthquake and Structures, Article vol. 10, no. 5, pp. 1013-1032. DOI: 10.12989/eas.2016.10.5.1013

[8] Guzel, Y., Rouainia, M., Elia, G. 2020. Effect of soil variability on nonlinear site response predictions: Application to the Lotung site, Computers and Geotechnics, vol. 121, Art. no. 103444. DOI: 10.1016/j.compgeo.2020.103444

[9] Elia, G. 2015. Site response for seismic hazard assessment, Encyclopedia of earthquake engineering, 2015. DOI: 10.1007/978-3-642-35344-4_241

[10] Amorosi, A., Boldini, D., di Lernia, A. 2017. Dynamic soil-structure interaction: A three-dimensional numerical approach and its application to the Lotung case study,

Computers and Geotechnics, vol. 90, pp. 34-54. DOI: 10.1016/j.compgeo.2018.02.002

[11] Salvati, L. A. Salvati, Pestana, J. M. 2006. Small-strain behavior of granular soils. II: Seismic response analyses and model evaluation, Journal of Geotechnical and Geoenvironmental Engineering, vol. 132, no. 8, pp. 1082-1090. DOI: 10.1061/(ASCE)10900241(2006)132:8(1082)

[12] Hallal, M. M., Cox, B. R. 2021. An H/V geostatistical approach for building pseudo-3D Vs models to account for spatial variability in ground response analyses Part I: Model development, Earthquake Spectra, vol. 37, no. 3, pp. 2013-2040. DOI: 10.1177/8755293020981989

[13] Seylabi, E., Hallal, M. M., Cox, B. R. 2022. Site characterization at Treasure Island and Delaney Park downhole arrays by heterogeneous data assimilation, Earthquake Spectra, vol. 38, no. 4, pp. 2398-2421. DOI: 10.1177/87552930221094060

[14] Tsai, C. C., Chang, W. S., Chiou, J. S. 2017. Enhancing prediction of ground response at the Turkey flat geotechnical array, Bulletin of the Seismological Society of America, vol. 107, no. 5, pp. 2043-2054. DOI:10.1785/0120160324

[15] Rubinstein, J. L. 2011. Nonlinear site response in medium magnitude earthquakes near Parkfield, California, Bulletin of the Seismological Society of America, vol. 101, no. 1, pp. 275-286. DOI: 10.1785/0120090396

[16] Dikmen, S. U., Edincliler, A., Pinar, A. 2015. Northern Aegean Earthquake (Mw=6.9): Observations at three seismic downhole arrays in Istanbul, Soil Dynamics and Earthquake Engineering, vol. 77, pp. 321-336. DOI: 10.1016/j.soildyn.2015.06.008[17] Kurtuluş, A. 2011. Istanbul geotechnical downhole arrays, Bulletin of Earthquake Engineering, vol. 9, no. 5, pp. 1443-1461. DOI: 10.1007/s10518-011-9268-0

[18] Turkish Building Earthquake Code (2018). Turkiye Bina Deprem Yonetmeligi, Deprem Etkisi Altında Binaların Tasarımı icin Esaslar.

[19] EC8, 2004. Design of structures for earthquake resistance—Part 1: General rules, seismic actions and rules for building, 2004.

[20] ESRI 2019. ArcGIS, ed. Redlands, CA: Environmental Systems Research Institute.

[21] Hashash, Y. M., Musgrove, M., Harmon, J. 2018. Nonlinear and equivalent linear seismic site response of one-dimensional soil columns: User Manual v7. 0, Deepsoil Software. University of Illinois at Urbana-Champaign.

[22] Seed, H.B. and Idriss, I.M. 1970. Soil moduli and damping factors for dynamic response analyses. Rep. No. EERC 70/10. Berkeley: Earthquake Engineering Research Center, University of California.

[23] Vucetic, M., Dobry, R. 1991. Effect of soil plasticity on cyclic response, Journal of geotechnical engineering, vol. 117, no. 1, pp. 89-107, 1991. DOI: 10.1061/(ASCE)07339410(1991)117:1(89)

[24] Kaklamanos, J., Bradley, B. A., Thomspon E. M., Baise, L. G. 2013. Critical Parameters Affecting Bias and Variability in SiteResponse Analyses Using KIK-net Downhole Array Data, Bulletin of the Seismological Society of America, vol. 103, 1733–1749. DOI: 10.1785/0120120166

[25] Zalachoris, G., Rathje, E. M. 2015. Evaluation of one-dimensional site response techniques using borehole arrays. Journal of Geotechnical and Geoenvironmental Engineering, vol. 141, no. 12. DOI: 10.1061/(ASCE)GT.1943-5606.0001366